White matter microsctructure predicts focal and broad functional dedifferentiation of visual processing in normal aging

Jenny R. Rieck, Ph.D. [a]
Karen M. Rodrigue, Ph.D. [b]
Denise C. Park, Ph.D. [b]
Kristen M. Kennedy, Ph.D. [b]

[a] Rotman Research Institute, Baycrest Health Sciences, Toronto, ON, M6A 2E1 CANADA
[b] Center for Vital Longevity, School of Behavioral and Brain Sciences, University of Texas at Dallas, Dallas, TX 75235, USA

Number of Pages: 30 Figures: 3 Tables: 3
Word Counts: Abstract: 238 Introduction: 778 Discussion: 14245

Updated : 9/22/2019

Abstract

Ventral visual cortex exhibits highly organized and selective patterns of functional activity associated with visual processing. However, this specialization decreases in normal aging, with functional responses to different visual stimuli becoming more similar, a phenomenon termed “dedifferentiation”. The current study tested the hypothesis that age-related degradation of the inferior longitudinal fasciculus (ILF), a white matter pathway involved in visual perception, could account for dedifferentiation of both localized and distributed brain activity in ventral visual cortex. Participants included 281 adults, ages 20-89, from the Dallas Lifespan Brain Study who underwent diffusion weighted imaging to measure white matter diffusivity and functional magnetic resonance imaging to measure functional activity selective to viewing photographs from different image categories (e.g., faces and houses). In general, decreased ILF anisotropy significantly predicted functional dedifferentiation in both face-selective fusiform gyrus and across the whole ventral visual cortex, beyond the effect of age. Specifically, there was a local effect of structure on function, such that anisotropy in a smaller mid-fusiform region of ILF predicted less selective (i.e., more dedifferentiated) response to viewing faces in a proximal face-responsive region of fusiform, whereas the whole ILF predicted less selective response across ventral visual cortex for viewing animate (e.g., human faces and animals) versus inanimate (e.g., houses and chairs) images. These results suggest decreased white matter anisotropy is associated with maladaptive differences in proximal brain function, and may be an important variable to consider when interpreting age-differences in functional activity.

Introduction

Ventral visual cortex encompasses regions of occipito-temporal cortex that are uniquely specialized for the identification and recognition of visual stimuli (Grill-Spector & Malach, 2004). Abundant early neuroimaging work has demonstrated selective and localized brain response when viewing certain categories of images (e.g., face-selective regions of fusiform gyrus; Kanwisher, McDermott, & Chun, 1997; Epstein, Harris, Stanley, & Kanwisher, 1999; Haxby et al., 1994), with further evidence for category-specific patterns of activity distributed broadly across ventral visual cortex (Haxby et al., 2001; O'Toole, Jiang, Abdi, & Haxby, 2005). Moreover, one of the largest distinctions in ventral visual cortex is characterized by activity in lateral and superior regions when viewing animate images (e.g., faces, animals, bodies) versus medial and inferior regions when viewing inanimate images (e.g., tools, houses; Grill-Spector & Weiner, 2014; Haxby et al., 2011; Proklova, Kaiser, & Peelen, 2016; Sha et al., 2014). Researchers have proposed that smaller, specialized regions, like face-selective fusiform, are responsible for narrow category distinctions (i.e., "face" vs. "house") and are nested within larger functional regions involved in superordinate distinctions (i.e., "animate" vs. "inanimate"; Grill-Spector & Weiner, 2014), suggesting that categorical representations in ventral visual cortex are multifaceted and exist at both a focal and broad level.

With advanced age, these highly specialized and unique representations associated with processing different visual stimuli become less distinct or "dedifferentiated" (Park et al., 2004; Grady et al., 1994; see Koen & Rugg, 2019 for a review). Specifically, localized regions of fusiform specialized for face processing show a broadened response by activating to non-face stimuli (Park et al., 2004; Park et al., 2012). Furthermore, the distributed patterns of brain activity when viewing faces versus other inanimate stimulus categories (e.g., houses or chairs)

become more similar in older age (Burianová, Lee, Grady, & Moscovitch, 2013; Carp, Park, Polk, & Park, 2011). Importantly, this neural dedifferentiation has been associated with poorer performance on measures of fluid processing (Park, Carp, Hebrank, Park, & Polk, 2010; Rieck, Rodrigue, Kennedy, Devous, & Park, 2015) and face-matching (Burianová et al., 2013), suggesting that individual differences in brain activity underlying visual perception may account for cognitive aging processes (Park & Reuter-Lorenz, 2009).

One possible explanation for dedifferentiation of functional activity in aging is degradation of the underlying white matter structure. Aging is characterized by dysmyelination and alteration of white matter fiber organization, which, in turn, likely interferes with the transfer and function of neural signals in gray matter (Barnes & McNaughton, 1980; Daselaar et al., 2015). Prior work has examined how measures of white matter microstructure explain age differences in: task-evoked functional response (Burzynska et al., 2013; de Chastelaine, Wang, Minton, Muftuler, & Rugg, 2011; Hakun, Zhu, Brown, Johnson, & Gold, 2015; Madden et al., 2007; Persson et al., 2006; Zhu, Johnson, Kim, & Gold, 2015; see Bennett & Rypma, 2013 and Warbrick, Rosenberg, & Shah, 2017 for reviews), modulation of functional response amplitude (Brown, Hakun, Zhu, Johnson, & Gold, 2015; Webb, Hoagey, Foster, Rodrigue, & Kennedy, *in press*), and functional connectivity between cortical regions (Chen, Chou, Song, & Madden, 2009; Davis, Kragel, Madden, & Cabeza, 2012). However, the impact of age-related white matter degradation on highly specialized functional activity (as found in the ventral visual cortex) is unclear.

Here we examine the impact of aging on the relationship between category-selective representations in ventral visual cortex and underlying microstructure of the inferior longitudinal fasciculus (ILF), the principal white matter pathway that connects occipital cortex to inferior

and medial temporal brain regions (Catani, Jones, Donato, & Ffytche, 2003). Previous work has identified ILF fibers that serve as direct connections between face-selective functional regions of ventral visual cortex (Gschwind, Pourtois, Schwartz, Van De Ville, & Vuilleumier, 2012; Pyles, Verstynen, Schneider, & Tarr, 2013; Weiner et al., 2016), suggesting that this white matter structure supports the specialized functional activity in ventral visual cortex.

We hypothesized that age-related degradation of ILF would account for functional dedifferentiation during visual processing at both the focal and distributed level. To test this hypothesis we utilized two indices of dedifferentiation, also referred to as "selectivity": (1) selectivity for faces in localized face-selective regions of fusiform gyrus (i.e., fusiform face area); and (2) broad selectivity for animacy across the entire ventral visual cortex. In general, functional selectivity describes the degree to which a specific region of cortex shows increased and selective response during one experimental condition (i.e., viewing faces) but not another (i.e., viewing houses). This hypothesis was tested in the Dallas Lifespan Brain Study, with adults ranging in age from 20-89 years, allowing the exploration of the relationship between white matter and neural dedifferentiation across the adult lifespan, including often excluded groups of middle-aged adults and very old age adults (i.e., > 80 years).

Methods

Participants

Participants consisted of a subsample from the Dallas Lifespan Brain Study (DLBS) who underwent passive-viewing functional magnetic resonance imaging (fMRI) and diffusion tensor imaging (DTI; $N = 299$). Participants' informed consent was obtained in accordance with protocol approved by the University of Texas at Dallas and the University of Texas

Southwestern Medical Center. Participants were screened to be right-handed and fluent English speakers with normal or corrected-to-normal vision (at least 20/30), and if necessary, vision was corrected using MRI-compatible corrective lenses during the fMRI session. Participants were additionally screened to be cognitively intact (Mini Mental Status Exam ≥ 26; Folstein, Folstein, & McHugh, 1975) with no history of neurological or psychiatric conditions, head trauma, drug or alcohol problems, or significant cardiovascular disease. Participants with outlier data points (detailed in *Statistical Analysis* section; *N*=18) for each neural measure were identified and excluded from analyses, resulting in a final sample size of 281 (see **Table 1** for sample demographics).

Table 1. *Sample demographics by decade*

Decade	N (% female)	Age	Years of Education	MMSE
20 – 29	41 (65.9%)	24.37 (2.78)	15.95 (2.32)	28.90 (1.26)
30 – 39	40 (60.0%)	34.06 (2.83)	16.85 (2.35)	28.63 (1.17)
40 – 49	41 (65.9%)	45.41 (3.19)	15.82 (1.99)	28.54 (1.19)
50 – 59	37 (73.0%)	54.63 (2.87)	16.89 (2.20)	28.76 (.925)
60 – 69	43 (58.1%)	64.82 (2.88)	16.88 (2.16)	28.21 (1.25)
70 – 79	39 (66.7%)	73.34 (2.75)	16.23 (2.40)	28.00 (1.29)
80 – 89	40 (60.0%)	83.65 (2.66)	16.28 (2.35)	27.30 (1.11)
Whole Sample	281 (64.1%)	54.23 (19.99)	16.41 (2.27)	28.33 (1.27)

Note. Data were analyzed with age as a continuous variable in all analyses. Mean (standard deviation); MMSE – Mini Mental State Exam

MRI acquisition.

Participants were scanned on a single Philips Achieva 3T whole body scanner equipped with an 8-channel head coil. DTI volumes were acquired with the following parameters: TR = 4410 ms; TE = 51 ms; flip angle = 90 ms; FOV = 224 x 149 x 224; XY matrix: 112 x 110; 50 slices per volume; 30 directions were acquired at b=1000 ms, plus a b0 non-diffusion weighted

image. Blood-oxygen-level dependent (BOLD) fMRI data were acquired using a T2*-weighted echo-planar imaging sequence with 43 interleaved axial slices (in a 64 × 64 matrix) acquired parallel to the anterior commissure-posterior commissure line with the following parameters: 3.4 × 3.4 × 3.5 mm^3 voxels, FOV = 220 mm, TE = 25 ms, TR = 2 sec, FA = 80°. High-resolution anatomical images (used to coregister anatomical masks to native diffusion and functional space) were collected with a T1-weighted MP-RAGE sequence with the following parameters: 160 sagittal slices, 1 × 1 × 1 mm^3 voxels; 256 × 256 × 160 matrix, FOV = 220 mm, TE = 3.76 ms, TR = 8.19 ms, FA = 12°.

Diffusion tensor imaging

DTI processing

Diffusion volumes were processed using the FMRIB's Diffusion Toolbox (FDT) in FSL (Behrens, Berg, Jbabdi, Rushworth, & Woolrich, 2007; Behrens et al., 2003). First, volumes underwent eddy current correction to correct for distortions caused by eddy currents in the gradient coils, as well as simple head motion during image acquisition by using an affine registration to a reference volume (using FLIRT). Second, the images were skull stripped using Brain Extraction Tool. Next, diffusion tensors were fit on corrected data using *dtifit* to create a voxel-wise map of the three primary diffusion directions (i.e., λ_1, λ_2, and λ_3) for each participant.

The three diffusion directions were used to compute our primary measure of white matter microstructure: fractional anisotropy (FA), which describes the ratio of diffusion in the primary direction ($\lambda 1$ or axial diffusivity; AD) relative to perpendicular directions (λ_2 and λ_3 or radial diffusivity; RD). Because FA is a composite index of diffusivity in all directions, it is important to consider axial and radial diffusivity interpreting differences in white matter microstructure (e.g., decreased axial diffusivity coupled with increased radial diffusivity could result in

decreased FA). Therefore, in the current study significant effects of FA were further explored by also examining the contribution of AD and RD to the statistical models.

Isolating white matter structures

The primary white matter pathway of interest was the inferior longitudinal fasciculus (ILF). Four additional white matter structures were identified to serve as control white matter regions: the superior longitudinal fasciculus (SLF), the uncinate fasciculus (UF), and the genu and splenium of the corpus callosum.

Probabilistic tractography was conducted to isolate the three bilateral association white matter pathways (ILF, SLF and UF), separately in each participant's native space using FDT in FSL (Behrens et al., 2007). First, diffusion parameters were estimated at each voxel using *bedpostX*, which generates a probability distribution function of the primary diffusion directions. Then, to determine connectivity between voxels, *probtrackX* was used to estimate the distribution of connections between the seed regions (i.e., origin) and waypoint (i.e., inclusion) regions (described below). The output from this step was a connectivity value for each voxel that represents the number of fibers that passed through that voxel.

All masks were constructed in standard Montreal Neurological Institute (MNI) space and then backwarped to each participant's native diffusion space; and all seed and waypoint regions were rectangular masks: 6 mm deep (anterior-posterior/coronal); 18 mm wide (left-right/sagittal) and 28 mm high (dorsal-ventral/axial), constructed separately for the left and right hemispheres. A midline exclusion mask was also included to eliminate fibers that crossed hemisphere.

ILF seed masks (i.e., tract origins) were created in occipital white matter, 24 mm anterior to the most posterior slice of the brain, and a single waypoint mask was created in temporal white matter, 50 mm anterior to the seed mask. Seed and waypoint masks were positioned such

that they were centered around anterior-posterior oriented white matter as evident on the MNI template (see Figure 1A for an illustration of ILF masks and the resulting pathway for a representative participant). For the SLF, seed masks were constructed in superior white matter on the most posterior coronal slices in which the splenium of the corpus callosum was visible on the MNI template. Two SLF waypoint masks were constructed 22 mm and 44 mm anterior to the seed mask. For the UF, seed masks were positioned in anterior temporal white matter, 30 mm posterior to the tip of the temporal pole. One waypoint mask was placed in the white matter of the anterior floor of the external capsule.

The resulting white matter tracts were thresholded at 15% of the maximum connectivity value, which ensured that tracts only included those voxels with a high likelihood of being connected to the seed and waypoint regions (following Bennett, Motes, Rao, & Rypma, 2012). All tracts were then visually inspected to verify that the backwarping of the seed and waypoint regions to native diffusion space resulted in proper tracking. Thresholded tracts were binarized, and mean FA, AD, and RD were extracted and averaged across hemispheres.

To localize fibers within the genu (anterior portion) and splenium (posterior portion) of the corpus callosum, rather than including pericallosal fibers, regions of interest were hand-traced on the T2-weighted (b0) baseline image for each participant in their native diffusion space with high reliability (intraclass correlation coefficient > .95). Each region was traced with a stylus on an LCD digitizing tablet using Analyze v12.0 software (Mayo Clinic, Rochester, MN). The genu and splenium were both traced on the slices in which they were optimally visible, for each participant with at least three slices included per structure. For each participant, diffusivity measure (e.g., FA, AD, RD) were extracted from the hand-traced genu and splenium and averaged across slices for each structure.

Functional magnetic resonance imaging

Visual stimuli and task design

While in-scanner, participants were instructed to view images from six categories: human faces, primates, cats, houses, chairs, and phase-scrambled control stimuli. Each category was composed of 64 grayscale photographs (400 pixels wide x 300 pixels tall), and cat stimuli were made up of 32 domestic cat and 32 wild cat photographs. The images of human faces were taken from our published face library (Kennedy, Hope, & Raz, 2009; Minear & Park, 2004). Animal photographs (primates, domestic cats, and wild cats) were taken from the internet and cropped so that the animal's face was clearly visible. Like the human faces, only animal images with front-facing and neutral expressions were chosen. Houses were photographed from various locations across the United States. The photographs of chairs were taken from furniture websites. Control images were created by scrambling the phase information in all the experimental stimuli so that the spatial frequency information was preserved, but the visual information was meaningless.

Visual stimuli were presented in a block design across two seven-minute runs. There was a 10-sec fixation screen at the beginning and end of each run to allow brain tissue magnetization to reach a steady state and to allow for participants to become acclimated to the noise of the scanner. Within each run, 24 blocks (four blocks from the six categories) were presented in pseudorandom order. Within each block there were eight images randomly selected from the same category so that each image was only presented one time. Individual images were presented for 2 seconds each with no inter-stimulus interval. Participants were not required to make any response during the scan, but were instructed to pay attention to each image. A subset of data from this task (i.e., the human and house viewing conditions) have been discussed in previous work (Park et al., 2012).

fMRI processing

Individual participant's time series data were preprocessed with Statistical Parametric Mapping 8 (SPM8; Wellcome Department of Cognitive Neurology, London, UK). First, images were corrected for differences in slice time acquisition. Next, individual volumes were corrected for within-run participant movement. Finally, images were smoothed with an isotropic 8 mm^3 full-width-half-maximum Gaussian kernel. For the current study, the primary analysis of the fMRI data was conducted in participant native-space to ensure the least amount of processing prior to analysis. However, an additional pipeline was run which included a spatial normalization to a standardized MNI template prior to the smoothing step in order to ensure that warping the data to a standard space did not differ from the analysis conducted in native space.

First-level statistics were conducted using the general linear model in SPM8 to model BOLD response to each of the six image categories viewed in scanner: human faces, primates, cats, houses, chairs, and scrambled. For the current study, additional first-level models were conducted to estimate neural response to animate (human, primate, and cat) and inanimate (house and chair) categories. In all models, motion parameters for each individual were also included as nuisance regressors to control for individual differences in movement across the scanning session. The resulting parameter estimates (β-weights) from the first-level models quantified how well functional activity in each voxel corresponded to a predicted neural response for that condition, thereby providing an estimate of BOLD response to each experimental condition.

Quantifying functional measures of dedifferentiation

For the current study, two indices of functional dedifferentiation, also referred to as "selectivity", were examined: (1) functional selectivity for faces in face-selective regions of

fusiform gyrus (e.g., fusiform face area); and (2) broad functional selectivity for animacy across the entire ventral visual cortex.

To quantify face selectivity, we focused on dedifferentiation in the fusiform face area (FFA), as this is the region of the core face-network that shows the strongest age-related dedifferentiation compared to other regions of the face network (e.g., occipital face area, superior temporal sulcus; Park et al., 2012). Following Park and colleagues (2012), for each participant, left and right FFA were identified within participant-native space by isolating a ~200 mm^2 contiguous region around the peak voxel in fusiform gyrus that evoked significant response to viewing human faces versus scrambled images (FFA voxels that have been mapped to a common space are illustrated in Figure 2C). Within the functionally defined FFA, neural selectivity was quantified as the average difference in neural response to human faces compared to houses (more details can be found in Park et al., 2012). For the current study, FFA selectivity measurements were averaged for left and right hemispheres.

A second index of selectivity was also computed based off prior work demonstrating widespread differences in functional representations associated with animacy (Grill-Spector & Weiner, 2014; Haxby et al., 2011; Proklova et al., 2016; Sha et al., 2014). For the current study, selectivity for animacy was quantified by calculating the similarity between neural response to animate images (human, primate and cat) and inanimate images (houses and chairs) using Euclidian distance, which is a measure of the magnitude of difference in neural response to different conditions across many voxels (Kriegeskorte, Mur, & Bandettini, 2008); a group-level contrast of animacy mapped to a common space is illustrated in Figure 2D).

Ventral visual cortex was identified for each participant using a participant-specific anatomical mask in conjunction with a functionally derived mask that isolated voxels in the

ventral visual mask that showed significant response to any of the visual stimuli. Specifically, an anatomical mask of the ventral visual pathway was backwarped to participant native-space using bilateral regions derived from the Automated Anatomical Labeling template (AAL; Tzourio-Mazoyer et al., 2002). These regions were selected to encompass all major structures in the ventral-temporal cortex (involved in the ventral visual pathway) and included: calcarine sulcus, cuneus, lingual gyrus, inferior occipital gyrus, fusiform gyrus, parahippocampal gyrus, inferior and middle temporal gyrus, and temporal pole. Second, a functional mask was generated for each individual to isolate voxels within the ventral visual pathway that were responsive to visual input. Following O'Toole and colleagues (2014), the functional mask was defined as those voxels within the ventral visual cortex that varied significantly across the six stimulus conditions as determined by an analysis of variance F-test. For the current study, the significance threshold was set to $p < .00001$ (O'Toole et al., 2014). To note, relaxing or increasing the significance threshold for the functional masks did not alter the results reported here.

Statistical analysis

Outliers were removed from the sample by identifying those participants with outlier data points for any of the three primary brain variables of interest: ILF FA; FFA face selectivity; and ventral visual animacy selectivity. To ensure outlier removal was not influenced by normal aging effects, first age was regressed out of each brain variable of interest. Outliers were identified as those data points outside 1.5 times the interquartile range for the standardized residuals (after accounting for age). Eighteen total outliers were identified (ILF FA, n= 5; face selectivity, n = 7; animacy selectivity outliers, n = 5; both face and animacy selectivity, n = 1), for a final sample of N = 281.

Using R (R Core Team), several hierarchical regression models were conducted in order to examine the predictive effect of white matter on the different functional measures of selectivity. For each hierarchical regression, age was entered first, followed by FA for the control white matter regions (i.e., SLF, UF, genu and splenium), and finally, ILF FA (the white matter pathway of interest). This analysis allowed us to determine if ILF microstructure predicted differences in functional selectivity beyond the effect of aging and controlling for white matter FA in other brain regions. Because the animacy measure was derived across a large region of ventral visual cortex in each individual's native space, the size of each individual's ventral visual area (as computed through their anatomically-derived mask; range = 4769-7744 voxels in size; mean number of voxels = 5893) was also included as a nuisance covariate in each model to ensure that results were not influenced by individual differences in ventral visual size. For models in which mean FA in ILF was found as a significant predictor, additional hierarchical regressions were conducted using other indicators of white matter diffusivity (i.e., axial and radial diffusivity) in order to determine which diffusion metrics accounted for the effect of FA.

Results

Age Effects on Structural and Functional Measures

Once the structural and functional measures were derived, the relationship of each marker to age was examined for sensitivity to general aging effects. As expected, with increasing age, diffusion in ILF was more isotropic as evident by the decrease in FA values (r = -.57, p < .001), suggesting that integrity in ILF degrades with increasing age (**Figure 1B**). Age-related decreases in FA were characterized by two different patterns in axial and radial diffusivities (**Figure 1C-D**). Specifically, participants age 20 to 51 show age-related increases in radial diffusivity (r = .31, p < .001) and slight decreases in axial diffusivity (r = -.32, p < .001). On the other hand,

participants ages 52 to 89 showed age-related increases in both radial (r = .42, p < .001) and axial diffusivities (r = .30, p < .001), which might be suggestive of a more severe pattern of degradation in adults over the age of 50 (Bennett, Madden, Vaidya, Howard, & Howard, 2010; Burzynska et al., 2010).

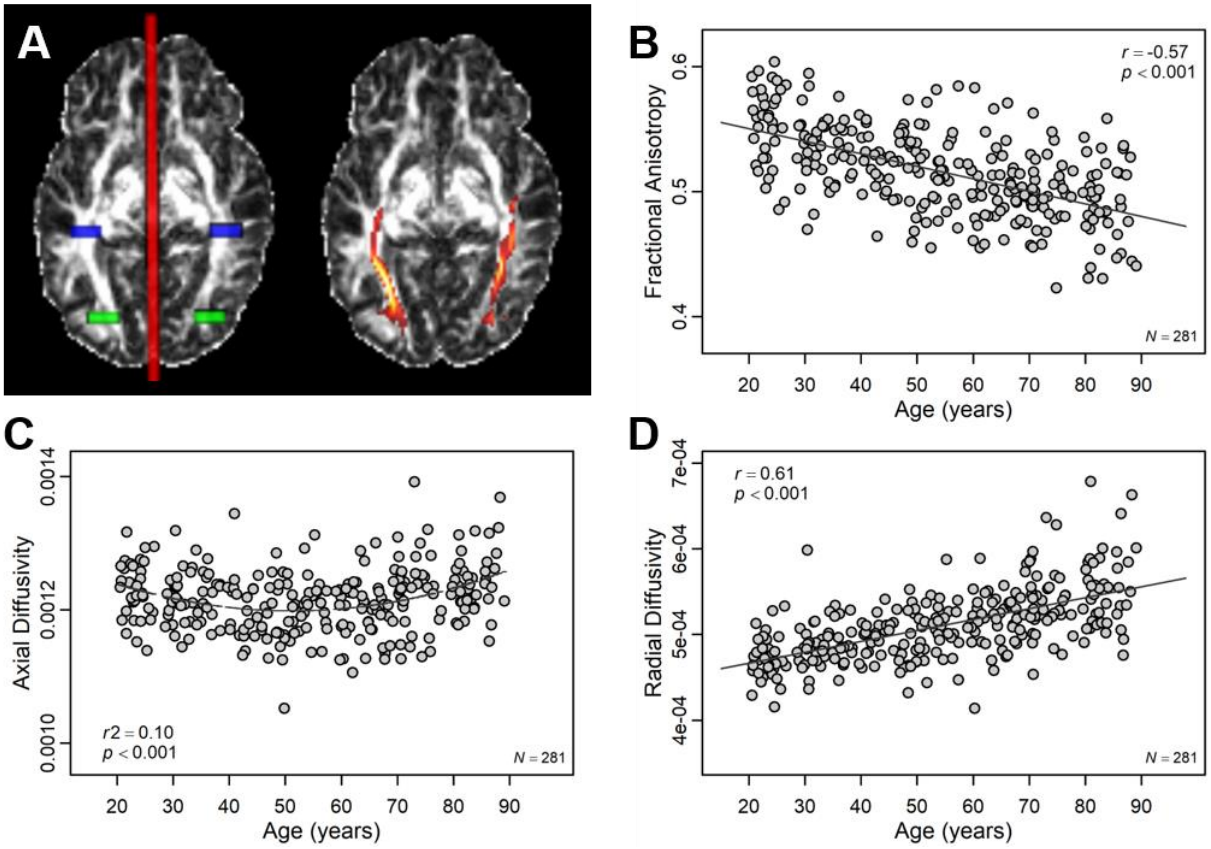

Figure 1. *Effect of age on white matter diffusion metrics in ILF*. (A) Seed (green), waypoint (blue), and exclusion (red) masks used for probabilistic tractography of left and right ILF (left image) as well as the resulting ILF tract (right image) are illustrated for a representative participant. (B) With increasing age, diffusivity in ILF was more isotropic (i.e., lower fractional anisotropy; which was characterized by (C) non-linear age-differences in axial diffusivity and (D) linear age increases in radial diffusivity.

Both functional measures of selectivity showed decreases with increasing age (**Figure 2**). Specifically, in face-selective regions of fusiform gyrus (e.g., FFA), the difference in neural response to faces compared to houses was decreased in older age (r = -.25, p < .001; Figure 2A).

Likewise, across the ventral visual cortex, the similarity of response between animate and inanimate images was decreased in older age (r = -.27, p < .001; Figure 2B).

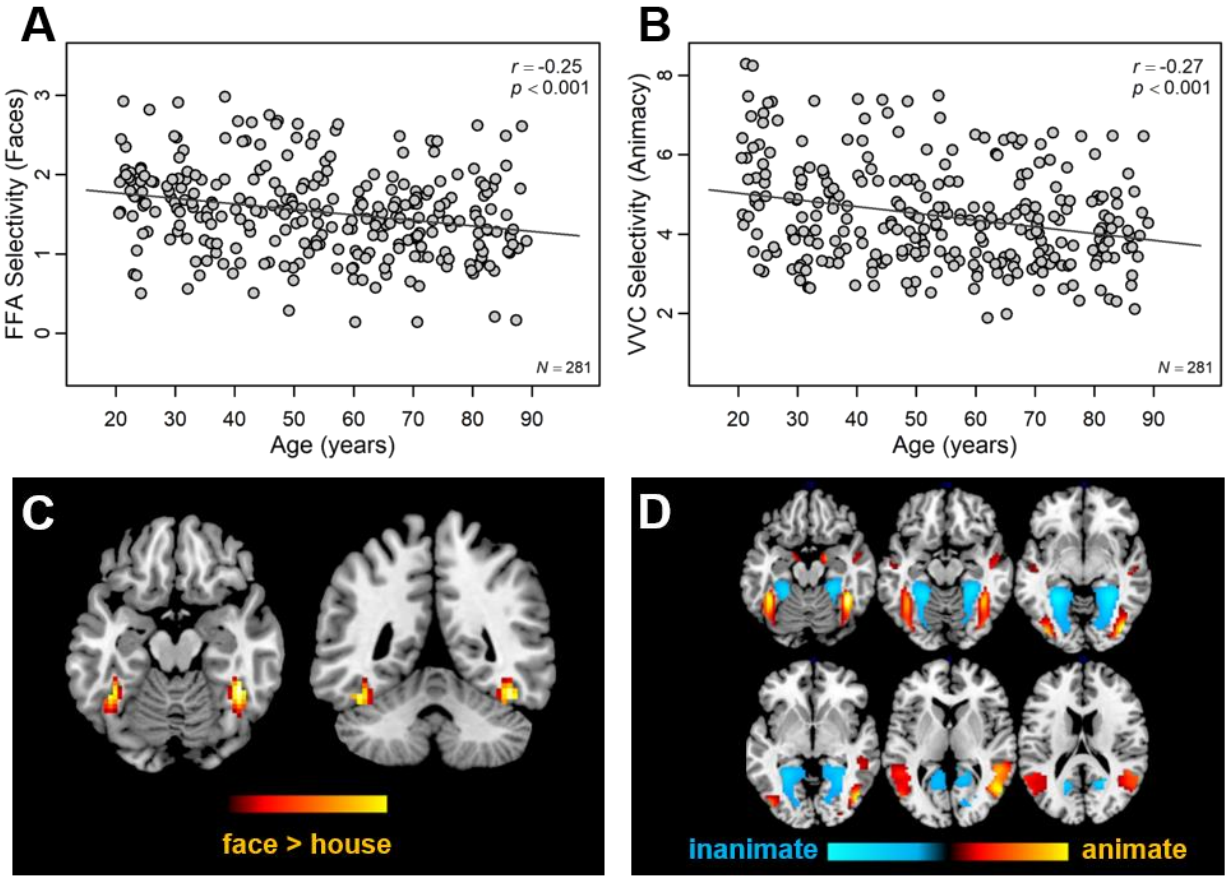

Figure 2: *Effect of age on neural selectivity*. (A) With increasing age, selectivity for faces in fusiform face area decreases. (B) Likewise, selectivity for animacy across ventral visual cortex (VVC) decreases. Functional activation maps illustrate (C) fusiform face area and (D) activity associated with viewing animate versus inanimate images mapped to a common template space.

Hierarchical regression models

Hierarchical regression models were conducted in which age and white matter metrics and nuisance covariates were entered to predict the two different measures of functional selectivity. The first set of models predicted selectivity for faces versus houses in FFA and found that older age predicted decreased face selectivity (ΔR^2 = .062, p<.001). However, adding mean FA of the ILF to the model (after controlling for age and FA in non-preferred white matter

pathways) did not significantly increase the amount of variance explained by the model (ΔR^2 = .002, p = .42; **Table 2A**).

Given that the ILF is a fairly long fiber pathway, (i.e., up to 10 cm in length; Catani et al., 2003) and the FFA regions identified in the current study were roughly 8 mm spheres, it is possible that the size-scale difference between the two measures accounted for the lack of the relationship between FA and face selectivity in FFA. Therefore, an additional regression model was conducted to determine if FA in a more local (i.e., mid-fusiform) portion of ILF was a better predictor of selectivity than FA averaged across the whole ILF pathway. For each individual, average FA was extracted for a 12 mm portion of ILF along the anterior-posterior axis that was centered around the y-coordinate for the group-level left (Y = -43) and right (Y = -48) FFA peaks respectively. Left and right regional FA were then averaged and entered in a hierarchical regression model (after age, control regions FA, and whole ILF FA) to predict selectivity for faces within FFA.

This additional analysis revealed that decreased FA within the mid-fusiform region of ILF predicted decreased face selectivity within FFA (β = 3.33), even when accounting for age, other white matter regions, and whole ILF FA (ΔR^2 = .022, p = .012). Two additional hierarchical regression models were conducted using axial and radial diffusivity, respectively, for each white matter region. These additional models demonstrated that the relationship between decreased white matter microstructure in mid-fusiform and decreased face selectivity in FFA was characterized by increased radial (ΔR^2 =.014, p = .041; **Table 2B**) and decreased axial diffusivities (ΔR^2 =.014 p = .044; **Table 2C**) when accounting for age and control region diffusivity measures.

Table 2. *Hierarchical regression model: Predicting selectivity for faces in FFA*

A. *Fractional Anisotropy (FA)*					
Model	Steps	Measurement	R^2	ΔR^2	ΔR^2 *p*-value
1	1	Age	**.062**	**.062**	**<.001**
2	1	Age	.068	.006	.797
	2	Other white matter pathways FA Sup. Long. Fasciculus Uncinate Fasciculus Genu, Splenium			
3	1	Age	.070	.002	.421
	2	Other white matter pathways FA			
	3	Whole ILF FA			
4	1	Age	**.092**	**.022**	**.012**
	2	Other white matter pathways FA			
	3	Whole ILF FA			
	4	Middle Fusiform ILF FA			
B. *Radial Diffusivity (RD)*					
Model	Steps	Measurement	R^2	ΔR^2	ΔR^2 *p*-value
1	1	Age Sup. Long. Fasciculus RD Uncinate Fasciculus RD Genu RD Splenium RD Whole ILF RD	**.081**	**.081**	**<.001**
2	1	Age Sup. Long. Fasciculus RD Uncinate Fasciculus RD Genu RD Splenium RD Whole ILF RD	**.095**	**.014**	**.041**
	2	Middle Fusiform ILF RD			
C. *Axial Diffusivity (AD)*					
Model	Steps	Measurement	R^2	ΔR^2	ΔR^2 *p*-value
1	1	Age Sup. Long. Fasciculus AD Uncinate Fasciculus AD Genu AD Splenium AD Whole ILF AD	**.085**	**.085**	**<.001**
2	1	Age Sup. Long. Fasciculus AD Uncinate Fasciculus AD Genu AD Splenium AD Whole ILF AD	**.099**	**.014**	**.044**
	2	Middle Fusiform ILF AD			

The second set of hierarchical regression models predicted selectivity for animacy across ventral visual cortex. As expected, age was a significant predictor of selectivity for animacy (ΔR^2 = .071, p <.001). Adding FA in control white matter regions (ΔR^2 = .006, p =.788) and ventral visual volume size (ΔR^2 = .001, p < .583) did not explain significantly more variance in neural selectivity. When accounting for all of these variables, whole ILF FA remained a significant predictor of neural selectivity for animacy (β = 10.70, ΔR^2 = .037, p < .001; **Table 3A**); specifically, decreased white matter FA in ILF predicted decreased selectivity across ventral visual cortex (see **Figure 3** for illustration of structure-function effects). As before, two additional hierarchical regression models were conducted using axial and radial diffusivity for each white matter region. These models indicated that decreased selectivity for animacy was predicted by increased radial diffusivity (ΔR^2 =.028, p < .01; **Table 3B**), with no relationship found for axial diffusivity (ΔR^2 =.001, p = .527; **Table 3C**).

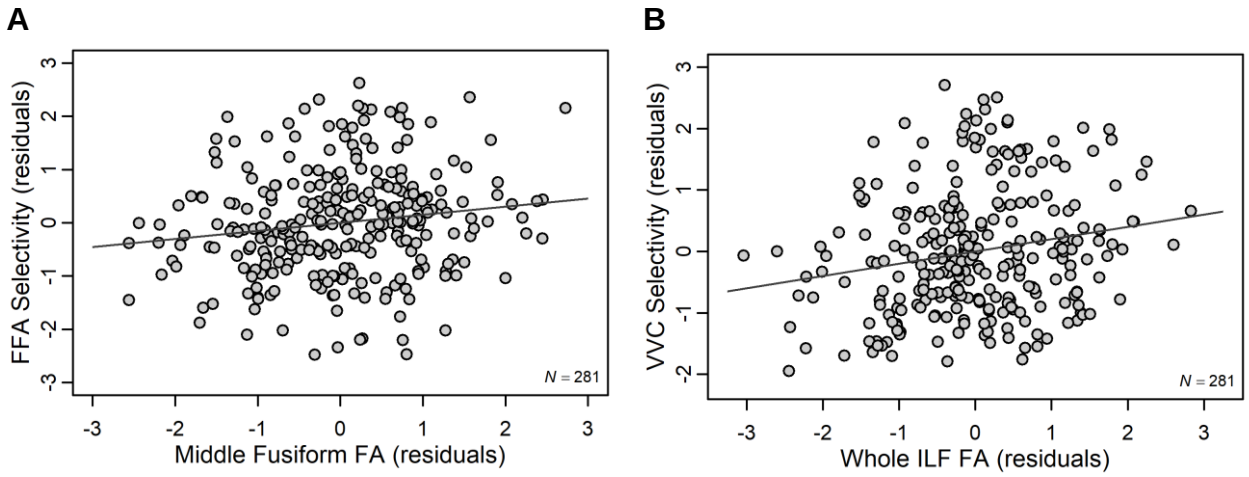

Figure 3. *Visualization of structure-functional relationships.* (A) Increased FA in a portion of middle-fusiform ILF corresponds to increased face-selectivity in fusiform face area (FFA). Standardized residuals (after accounting for age, and other white matter tracts) are plotted for middle-fusiform FA and FFA selectivity. (B) Increased FA across the entire ILF corresponds to increased selectivity for animacy across ventral visual cortex (VVC). Standardized residuals (after accounting for age, other white matter tracts, and ventral visual size) are plotted for whole ILF FA and ventral visusal selectivity for animacy.

Table 3. *Hierarchical regression model: Predicting selectivity for animacy across VVC*

A. *Fractional Anisotropy (FA)*					
Model	Steps	Measurement	R^2	ΔR^2	ΔR^2 *p*-value
1	1	Age	**.071**	**.071**	**<.001**
2	1	Age	.077	.006	.788
	2	Other white matter pathways FA Sup. Long. Fasciculus Uncinate Fasciculus Genu, Splenium			
3	1	Age	.078	.001	.583
	2	Other white matter pathways FA			
	3	Ventral visual cortex size			
4	1	Age	**.115**	**.037**	**.001**
	2	Other white matter pathways FA			
	3	Ventral visual cortex size			
	4	ILF FA			
B. *Radial Diffusivity (RD)*					
Model	Steps	Measurement	R^2	ΔR^2	ΔR^2 *p*-value
1	1	Age	.094	**.094**	**<.001**
		Sup. Long. Fasciculus RD			
		Uncinate Fasciculus RD			
		Genu RD			
		Splenium RD			
		Ventral visual cortex size			
2	1	Age	**.123**	**.028**	**.003**
		Sup. Long. Fasciculus RD			
		Uncinate Fasciculus RD			
		Genu RD			
		Splenium RD			
		Ventral visual cortex size			
	2	ILF RD			
C. *Axial Diffusivity (AD)*					
Model	Steps	Measurement	R^2	ΔR^2	ΔR^2 *p*-value
1	1	Age	**.116**	**.116**	**<.001**
		Sup. Long. Fasciculus AD			
		Uncinate Fasciculus AD			
		Genu AD			
		Splenium AD			
		Ventral visual cortex size			
2	1	Age	**.117**	**.001**	**.527**
		Sup. Long. Fasciculus AD			
		Uncinate Fasciculus AD			
		Genu AD			
		Splenium AD			
		Ventral visual cortex size			
	2	ILF AD			

Discussion

This work provides new evidence of a direct relationship between ILF microstructure properties and functional selectivity in ventral visual cortex during visual perception. Specifically, decreased white matter anisotropy in ILF corresponded to less selective activation for animacy across the ventral visual cortex, independent of the effect of age. This effect was not found when trying to predict neural selectivity for faces within a specialized region of the face processing network. However, white matter anisotropy within a smaller and more localized portion of the ILF did predict functional selectivity in fusiform face area. These results suggest that whole ILF white matter may be a stronger predictor of broad differences in selectivity across the entire ventral visual cortex, whereas more focal regions of ILF may be a stronger predictor of dedifferentiation of specialized face processing.

Whole ILF microstructure predicts broad but not focal measures of neural selectivity

The ILF is a fairly long fiber pathway that interconnects many areas of cortex between the occipital and temporal poles (Catani et al., 2003)—essentially along what is considered the ventral visual stream—and it is clear from behavioral studies that the ILF is important for a variety of different visually-related cognitive processes including: reading ability (Ellmore et al., 2010; Yeatman, Dougherty, Myall, Wandell, & Feldman, 2012), recognition of visual stimuli (Davis et al., 2009; Sasson, Doniger, Pasternak, & Assaf, 2010; Tavor et al., 2014), and speed of processing (Bennett et al., 2012; Turken et al., 2008). Yet, it is only recently that researchers have examined how white matter integrity in ILF relates to functional activity during visual processing. Both Gschwind et al., (2012) and Pyles et al., (2013) report that white matter fibers connecting specialized regions of the face-processing network overlap with a portion of the ILF,

suggesting that some fibers within ILF are important for transmitting neural activity related to face perception.

However, in the current study, no relationship was found between face-selectivity in fusiform face area and average FA of the entire ILF pathway, suggesting simply averaging the values for the entire tract—a common practice in DTI work (Bennett et al., 2012; Burzynska et al., 2010)—may not be the most sensitive predictor of brain activity within a small and localized region of the ventral visual pathway. Rather, FA within a more proximal region of ILF (mid-fusiform gyrus) was found to be the best predictor of face selectivity within FFA, suggesting that fibers within middle-fusiform portions of the ILF may subserve specialized neural activity in face-selective regions of cortex. On the other hand, whole ILF FA was found to be a significant predictor of selectivity for animacy across a large area of ventral visual cortex. Therefore, as a whole, white matter fibers of the ILF may subserve basic visual processing involved in superordinate category distinction within ventral visual pathway. Together, these results suggest that white matter exerts a local effect on neural activity, such that higher anisotropy in a small portion of ILF better predicts functional activity in proximal regions of cortex, whereas the entire ILF predicts broad differences in activity across ventral visual cortex.

Different properties of white matter microstructure predict functional selectivity

The current study used mean tract fractional anisotropy (FA) as the primary index of white matter microstructure to predict functional selectivity. FA is a scalar measure that describes the relationship between the rates of water diffusion parallel to the primary direction of diffusion (axial diffusivity) relative to diffusion in perpendicular directions (radial diffusivity). Therefore, while FA is a useful measure for describing overall shape and orientation of diffusion, it is also interesting to consider how changes in both primary (axial) and perpendicular (radial)

diffusivity may be accounting for differences in FA. In general, studies examining effects of age on white matter find that age-related decreases in FA can be due to relative changes in both axial and radial diffusion. Specifically, decreased FA has been accounted for by three different patterns: (1) increased radial diffusivity only, which may indicate dysmyelination of the axonal sheath; (2) increased radial and axial diffusivity, which may indicate a more severe dysmyelination; and (3) increased radial and substantial decreases in axial diffusivity, which may indicate damage to the white matter axons (Bennett et al., 2010), although it is important to keep in mind that these are proxy metrics.

In the current study, decreased FA in middle-fusiform ILF predicted decreased selectivity for faces in FFA, and additional analyses found that decreased selectivity was also predicted by increased radial and decreased axial diffusivities (pattern #3), independent of the effect of age. This pattern of increased radial and decreased axial diffusivity may indicate that face selectivity in fusiform is sensitive to the pattern of diffusivity in nearby white matter which may be characterized by alterations to axonal cellular boundaries. These results suggest that white matter in middle-fusiform ILF may be more susceptible to more severe forms of degradation, and this in turn may impede functional response in nearby cortex. On the other hand, only increased radial diffusivity in whole ILF (pattern #1) was sensitive to decreased selectivity for animacy across ventral visual cortex, suggesting that dedifferentiation on a broader scale may be predicted by dysmyelination of ILF white matter fibers. To note, all of the associations between white matter metrics and neural selectivity persisted beyond the effect of age, therefore differences in diffusivity likely represent individual differences in white matter microstructure, rather than age-related degradation alone.

Interpreting the current results in the context of prior DTI-fMRI aging studies

Prior studies examining the effect of age on the relationship between white matter microstructure and functional activity have largely examined how white matter is related to changes in magnitude or modulation of BOLD response during a cognitive task, with the largest focus on frontal regions of the brain (see Bennett & Rypma, 2013 for a review). Researchers generally report that decreased frontal white matter integrity in older adults corresponds with overactivation of frontal cortex (Burzynska et al., 2013; Daselaar et al., 2015; Davis et al., 2012; de Chastelaine et al., 2011; Hakun et al., 2015; Madden et al., 2007; Persson et al., 2006; but see also de Chastelaine et al., 2011 and Davis et al., 2012 for opposite findings), suggesting that the general age-phenomenon of increased activity in frontal cortex may be a compensatory response to impaired white matter degradation (Daselaar et al., 2015). White matter degradation in older adults has also been associated with failures to deactivate default regions during task (Brown et al., 2015) and failure to up-modulate prefrontal activity in response to increasing task demands (Webb et al., in press).

We extend this prior work on higher-level cognition by moving our focus to structure-function relationships in ventral visual cortex during a basic perceptual task. Due to the highly organized and hierarchical nature of visual representations in ventral visual cortex (Grill-Spector & Weiner, 2014), we were able to target both focal (i.e., fusiform face area) and broad patterns of specialized functional activity. We report that dedifferentiation of functional response (i.e., less selective response) could be accounted for by decreased FA in underlying white matter at both fine-grain and coarse scales. This finding, in conjunction with prior DTI-fMRI studies, may indicate that decreased white matter connectivity predicts maladaptive alterations in brain function, be it decreased selectivity, frontal over-recruitment, or failure to modulate functional

activity. Therefore, underlying white matter structure is an important variable to consider when interpreting age-differences in brain function.

Conclusions

In sum, the present study offers the first examination of how white matter microstructure (through multiple white matter indices) in the ILF predicts functional selectivity in the ventral visual cortex across the entire adult lifespan. This study provides a comprehensive view of the relationship between measures of white matter microstructure and selectivity in a healthy, aging population, which may help dissociate normal from pathological brain aging in future studies. There are several important points to take away from these findings. First, the effect of white matter on functional selectivity appears to be local, such that neural activity is best predicted by integrity in nearby white matter. Specifically, whole ILF predicts selectivity for animacy across the entire ventral visual cortex, whereas a smaller, proximal region of ILF predicts selectivity for faces in a focal region of fusiform gyrus. Next, selectivity in fusiform face area is predicted by a more severe pattern of white matter degradation, specifically decreased axial and increased radial diffusivities, which may indicate that function in highly specialized regions of ventral visual cortex is susceptible to greater disruptions in nearby white matter connections. Future longitudinal studies directly examining intra-indiviudal changes in white matter tracts in relation to functional brain activation are needed to confirm the cross-sectional findings reported here.

Acknowledgments

This study was supported in part by National Institutes of Health grants: R37-AG-006265 (DCP); R37-AG-006265-S1 (DCP); R01-AG-056535 (KMK); R01-AG-057537 (KMR).

References

Barnes, C. A., & McNaughton, B. L. (1980). Physiological compensation for loss of afferent synapses in rat hippocampal granule cells during senescence. *The Journal of Physiology*, *309*, 473–485. https://doi.org/10.1113/jphysiol.1980.sp013521

Behrens, T. E. J., Berg, H. J., Jbabdi, S., Rushworth, M. F. S., & Woolrich, M. W. (2007). Probabilistic diffusion tractography with multiple fibre orientations: What can we gain? *NeuroImage*, *34*(1), 144–155. https://doi.org/10.1016/j.neuroimage.2006.09.018

Behrens, T. E. J., Woolrich, M. W., Jenkinson, M., Johansen-Berg, H., Nunes, R. G., Clare, S., … Smith, S. M. (2003). Characterization and propagation of uncertainty in diffusion-weighted MR imaging. *Magnetic Resonance in Medicine*, *50*(5), 1077–1088. https://doi.org/10.1002/mrm.10609

Bennett, I. J., Madden, D. J., Vaidya, C. J., Howard, D. V., & Howard, J. H. (2010). Age-related differences in multiple measures of white matter integrity: A diffusion tensor imaging study of healthy aging. *Human Brain Mapping*, *31*(3), 378–390. https://doi.org/10.1002/hbm.20872

Bennett, I. J., Motes, M. A., Rao, N. K., & Rypma, B. (2012). White matter tract integrity predicts visual search performance in young and older adults. *Neurobiology of Aging*, *33*(2), 433.e21-433.e31. https://doi.org/10.1016/j.neurobiolaging.2011.02.001

Bennett, I. J., & Rypma, B. (2013). Advances in functional neuroanatomy: A review of combined DTI and fMRI studies in healthy younger and older adults. *Neuroscience & Biobehavioral Reviews*, *37*(7), 1201–1210. https://doi.org/10.1016/j.neubiorev.2013.04.008

Brown, C. A., Hakun, J. G., Zhu, Z., Johnson, N. F., & Gold, B. T. (2015). White matter microstructure contributes to age-related declines in task-induced deactivation of the default mode network. *Frontiers in Aging Neuroscience*, *7*, 194. https://doi.org/10.3389/fnagi.2015.00194

Burianová, H., Lee, Y., Grady, C. L., & Moscovitch, M. (2013). Age-related dedifferentiation and compensatory changes in the functional network underlying face processing. *Neurobiology of Aging*, *34*(12), 2759–2767. https://doi.org/10.1016/j.neurobiolaging.2013.06.016

Burzynska, A. Z., Preuschhof, C., Bäckman, L., Nyberg, L., Li, S.-C., Lindenberger, U., & Heekeren, H. R. (2010). Age-related differences in white matter microstructure: Region-specific patterns of diffusivity. *NeuroImage*, *49*(3), 2104–2112. https://doi.org/10.1016/j.neuroimage.2009.09.041

Burzynska, Agnieszka Z., Garrett, D. D., Preuschhof, C., Nagel, I. E., Li, S.-C., Bäckman, L., … Lindenberger, U. (2013). A Scaffold for Efficiency in the Human Brain. *Journal of Neuroscience*, *33*(43), 17150–17159. https://doi.org/10.1523/JNEUROSCI.1426-13.2013

Carp, J., Park, J., Polk, T. A., & Park, D. C. (2011). Age differences in neural distinctiveness revealed by multi-voxel pattern analysis. *NeuroImage*, *56*(2), 736–743. https://doi.org/10.1016/j.neuroimage.2010.04.267

Catani, M., Jones, D. K., Donato, R., & Ffytche, D. H. (2003). Occipito-temporal connections in the human brain. *Brain*, *126*(9), 2093–2107. https://doi.org/10.1093/brain/awg203

Chen, N., Chou, Y., Song, A. W., & Madden, D. J. (2009). Measurement of spontaneous signal fluctuations in fMRI: Adult age differences in intrinsic functional connectivity. *Brain Structure and Function*, *213*(6), 571–585. https://doi.org/10.1007/s00429-009-0218-4

Daselaar, S. M., Iyengar, V., Davis, S. W., Eklund, K., Hayes, S. M., & Cabeza, R. E. (2015). Less Wiring, More Firing: Low-Performing Older Adults Compensate for Impaired White Matter with Greater Neural Activity. *Cerebral Cortex*, *25*(4), 983–990. https://doi.org/10.1093/cercor/bht289

Davis, S. W., Dennis, N. A., Buchler, N. G., White, L. E., Madden, D. J., & Cabeza, R. (2009). Assessing the effects of age on long white matter tracts using diffusion tensor tractography. *NeuroImage*, *46*(2), 530–541. https://doi.org/10.1016/j.neuroimage.2009.01.068

Davis, S. W., Kragel, J. E., Madden, D. J., & Cabeza, R. (2012). The Architecture of Cross-Hemispheric Communication in the Aging Brain: Linking Behavior to Functional and Structural Connectivity. *Cerebral Cortex*, *22*(1), 232–242. https://doi.org/10.1093/cercor/bhr123

de Chastelaine, M., Wang, T. H., Minton, B., Muftuler, L. T., & Rugg, M. D. (2011). The Effects of Age, Memory Performance, and Callosal Integrity on the Neural Correlates of Successful Associative Encoding. *Cerebral Cortex*, *21*(9), 2166–2176. https://doi.org/10.1093/cercor/bhq294

Ellmore, T. M., Beauchamp, M. S., Breier, J. I., Slater, J. D., Kalamangalam, G. P., O'Neill, T. J., … Tandon, N. (2010). Temporal lobe white matter asymmetry and language laterality in epilepsy patients. *NeuroImage*, *49*(3), 2033–2044. https://doi.org/10.1016/j.neuroimage.2009.10.055

Epstein, R., Harris, A., Stanley, D., & Kanwisher, N. (1999). The Parahippocampal Place Area: Recognition, Navigation, or Encoding? *Neuron*, *23*(1), 115–125. https://doi.org/10.1016/S0896-6273(00)80758-8

Folstein, M. F., Folstein, S. E., & McHugh, P. R. (1975). "Mini-mental state". A practical method for grading the cognitive state of patients for the clinician. *Journal of Psychiatric Research*, *12*(3), 189–198. https://doi.org/10.1016/0022-3956(75)90026-6

Grady, C. L., Maisog, J. M., Horwitz, B., Ungerleider, L. G., Mentis, M. J., Salerno, J. A., … Haxby, J. V. (1994). Age-related changes in cortical blood flow activation during visual processing of faces and location. *Journal of Neuroscience*, *14*(3), 1450–1462. https://doi.org/10.1523/JNEUROSCI.14-03-01450.1994

Grill-Spector, K., & Malach, R. (2004). The Human Visual Cortex. *Annual Review of Neuroscience*, *27*(1), 649–677. https://doi.org/10.1146/annurev.neuro.27.070203.144220

Grill-Spector, K., & Weiner, K. S. (2014). The functional architecture of the ventral temporal cortex and its role in categorization. *Nature Reviews Neuroscience*, *15*(8), 536–548. https://doi.org/10.1038/nrn3747

Gschwind, M., Pourtois, G., Schwartz, S., Van De Ville, D., & Vuilleumier, P. (2012). White-matter connectivity between face-responsive regions in the human brain. *Cerebral Cortex (New York, N.Y.: 1991)*, *22*(7), 1564–1576. https://doi.org/10.1093/cercor/bhr226

Hakun, J. G., Zhu, Z., Brown, C. A., Johnson, N. F., & Gold, B. T. (2015). Longitudinal alterations to brain function, structure, and cognitive performance in healthy older adults: A fMRI-DTI study. *Neuropsychologia*, *71*, 225–235. https://doi.org/10.1016/j.neuropsychologia.2015.04.008

Haxby, James V., Gobbini, M. I., Furey, M. L., Ishai, A., Schouten, J. L., & Pietrini, P. (2001). Distributed and Overlapping Representations of Faces and Objects in Ventral Temporal Cortex. *Science*, *293*(5539), 2425–2430. https://doi.org/10.1126/science.1063736

Haxby, James V., Guntupalli, J. S., Connolly, A. C., Halchenko, Y. O., Conroy, B. R., Gobbini, M. I., … Ramadge, P. J. (2011). A Common, High-Dimensional Model of the Representational Space in Human Ventral Temporal Cortex. *Neuron*, *72*(2), 404–416. https://doi.org/10.1016/j.neuron.2011.08.026

Haxby, James V., Horwitz, B., Ungerleider, L. G., Maisog, J. M., Pietrini, P., & Grady, C. L. (1994). The functional organization of human extrastriate cortex: A PET-rCBF study of selective attention to faces and locations. *Journal of Neuroscience*, *14*(11), 6336–6353. https://doi.org/10.1523/JNEUROSCI.14-11-06336.1994

Kanwisher, N., McDermott, J., & Chun, M. M. (1997). The Fusiform Face Area: A Module in Human Extrastriate Cortex Specialized for Face Perception. *Journal of Neuroscience*, *17*(11), 4302–4311. https://doi.org/10.1523/JNEUROSCI.17-11-04302.1997

Kennedy, K. M., Hope, K., & Raz, N. (2009). Life Span Adult Faces: Norms for Age, Familiarity, Memorability, Mood, and Picture Quality. *Experimental Aging Research*, *35*(2), 268–275. https://doi.org/10.1080/03610730902720638

Koen, J. D., & Rugg, M. D. (2019). Neural Dedifferentiation in the Aging Brain. *Trends in Cognitive Sciences*, *23*(7), 547–559. https://doi.org/10.1016/j.tics.2019.04.012

Kriegeskorte, N., Mur, M., & Bandettini, P. A. (2008). Representational similarity analysis—Connecting the branches of systems neuroscience. *Frontiers in Systems Neuroscience*, *2*. https://doi.org/10.3389/neuro.06.004.2008

Madden, D. J., Spaniol, J., Whiting, W. L., Bucur, B., Provenzale, J. M., Cabeza, R., … Huettel, S. A. (2007). Adult age differences in the functional neuroanatomy of visual attention: A

combined fMRI and DTI study. *Neurobiology of Aging*, *28*(3), 459–476. https://doi.org/10.1016/j.neurobiolaging.2006.01.005

Minear, M., & Park, D. C. (2004). A lifespan database of adult facial stimuli. *Behavior Research Methods, Instruments, & Computers*, *36*(4), 630–633. https://doi.org/10.3758/BF03206543

O'Toole, A. J., Jiang, F., Abdi, H., & Haxby, J. V. (2005). Partially Distributed Representations of Objects and Faces in Ventral Temporal Cortex. *Journal of Cognitive Neuroscience*, *17*(4), 580–590. https://doi.org/10.1162/0898929053467550

O'Toole, A. J., Natu, V., An, X., Rice, A., Ryland, J., & Phillips, P. J. (2014). The neural representation of faces and bodies in motion and at rest. *NeuroImage*, *91*, 1–11. https://doi.org/10.1016/j.neuroimage.2014.01.038

Park, D. C., Polk, T. A., Park, R., Minear, M., Savage, A., & Smith, M. R. (2004). Aging reduces neural specialization in ventral visual cortex. *Proceedings of the National Academy of Sciences*, *101*(35), 13091–13095. https://doi.org/10.1073/pnas.0405148101

Park, D. C., & Reuter-Lorenz, P. (2009). The Adaptive Brain: Aging and Neurocognitive Scaffolding. *Annual Review of Psychology*, *60*(1), 173–196. https://doi.org/10.1146/annurev.psych.59.103006.093656

Park, J., Carp, J., Hebrank, A., Park, D. C., & Polk, T. A. (2010). Neural Specificity Predicts Fluid Processing Ability in Older Adults. *Journal of Neuroscience*, *30*(27), 9253–9259. https://doi.org/10.1523/JNEUROSCI.0853-10.2010

Park, J., Carp, J., Kennedy, K. M., Rodrigue, K. M., Bischof, G. N., Huang, C.-M., … Park, D. C. (2012). Neural Broadening or Neural Attenuation? Investigating Age-Related Dedifferentiation in the Face Network in a Large Lifespan Sample. *Journal of Neuroscience*, *32*(6), 2154–2158. https://doi.org/10.1523/JNEUROSCI.4494-11.2012

Persson, J., Nyberg, L., Lind, J., Larsson, A., Nilsson, L.-G., Ingvar, M., & Buckner, R. L. (2006). Structure–Function Correlates of Cognitive Decline in Aging. *Cerebral Cortex*, *16*(7), 907–915. https://doi.org/10.1093/cercor/bhj036

Proklova, D., Kaiser, D., & Peelen, M. V. (2016). Disentangling Representations of Object Shape and Object Category in Human Visual Cortex: The Animate–Inanimate Distinction. *Journal of Cognitive Neuroscience*, *28*(5), 680–692. https://doi.org/10.1162/jocn_a_00924

Pyles, J. A., Verstynen, T. D., Schneider, W., & Tarr, M. J. (2013). Explicating the Face Perception Network with White Matter Connectivity. *PLOS ONE*, *8*(4), e61611. https://doi.org/10.1371/journal.pone.0061611

Rieck, J. R., Rodrigue, K. M., Kennedy, K. M., Devous, M. D., & Park, D. C. (2015). The effect of beta-amyloid on face processing in young and old adults: A multivariate analysis of

the BOLD signal. *Human Brain Mapping*, *36*(7), 2514–2526. https://doi.org/10.1002/hbm.22788

Sasson, E., Doniger, G. M., Pasternak, O., & Assaf, Y. (2010). Structural correlates of memory performance with diffusion tensor imaging. *NeuroImage*, *50*(3), 1231–1242. https://doi.org/10.1016/j.neuroimage.2009.12.079

Sha, L., Haxby, J. V., Abdi, H., Guntupalli, J. S., Oosterhof, N. N., Halchenko, Y. O., & Connolly, A. C. (2014). The Animacy Continuum in the Human Ventral Vision Pathway. *Journal of Cognitive Neuroscience*, *27*(4), 665–678. https://doi.org/10.1162/jocn_a_00733

Tavor, I., Yablonski, M., Mezer, A., Rom, S., Assaf, Y., & Yovel, G. (2014). Separate parts of occipito-temporal white matter fibers are associated with recognition of faces and places. *NeuroImage*, *86*, 123–130. https://doi.org/10.1016/j.neuroimage.2013.07.085

Turken, U., Whitfield-Gabrieli, S., Bammer, R., Baldo, J. V., Dronkers, N. F., & Gabrieli, J. D. E. (2008). Cognitive processing speed and the structure of white matter pathways: Convergent evidence from normal variation and lesion studies. *NeuroImage*, *42*(2), 1032–1044. https://doi.org/10.1016/j.neuroimage.2008.03.057

Tzourio-Mazoyer, N., Landeau, B., Papathanassiou, D., Crivello, F., Etard, O., Delcroix, N., … Joliot, M. (2002). Automated Anatomical Labeling of Activations in SPM Using a Macroscopic Anatomical Parcellation of the MNI MRI Single-Subject Brain. *NeuroImage*, *15*(1), 273–289. https://doi.org/10.1006/nimg.2001.0978

Warbrick, T., Rosenberg, J., & Shah, N. J. (2017). The relationship between BOLD fMRI response and the underlying white matter as measured by fractional anisotropy (FA): A systematic review. *NeuroImage*, *153*, 369–381. https://doi.org/10.1016/j.neuroimage.2016.12.075

Webb, C. E., Hoagey, D. A., Foster, C. M., Rodrigue, K. M., Kennedy, K. M. (in press). Contributions of BOLD modulation and white matter diffusivity to cognitive aging: A lifespan SEM study. *Cerebral Cortex*, doi: 10.1093/cercor/bhz193.

Weiner, K. S., Jonas, J., Gomez, J., Maillard, L., Brissart, H., Hossu, G., … Rossion, B. (2016). The Face-Processing Network Is Resilient to Focal Resection of Human Visual Cortex. *Journal of Neuroscience*, *36*(32), 8425–8440. https://doi.org/10.1523/JNEUROSCI.4509-15.2016

Yeatman, J. D., Dougherty, R. F., Myall, N. J., Wandell, B. A., & Feldman, H. M. (2012). Tract Profiles of White Matter Properties: Automating Fiber-Tract Quantification. *PLOS ONE*, *7*(11), e49790. https://doi.org/10.1371/journal.pone.0049790

Zhu, Z., Johnson, N. F., Kim, C., & Gold, B. T. (2015). Reduced Frontal Cortex Efficiency is Associated with Lower White Matter Integrity in Aging. *Cerebral Cortex*, *25*(1), 138–146. https://doi.org/10.1093/cercor/bht212